Design of a 40-nm CMOS integrated on-chip oscilloscope for 5-50 GHz spin wave characterization

Cite as: AIP Advances **8**, 056001 (2018); https://doi.org/10.1063/1.5007435
Submitted: 02 October 2017 . Accepted: 06 October 2017 . Published Online: 01 December 2017

Eugen Egel, György Csaba, Andreas Dietz, Stephan Breitkreutz-von Gamm, Johannes Russer, Peter Russer, Franz Kreupl, and Markus Becherer

Design of a 40-nm CMOS integrated on-chip oscilloscope for 5-50 GHz spin wave characterization

Eugen Egel,[1,a] György Csaba,[2] Andreas Dietz,[1]
Stephan Breitkreutz-von Gamm,[1] Johannes Russer,[3]
Peter Russer,[3] Franz Kreupl,[1] and Markus Becherer[3]
[1]*Chair of Technical Electronics, Technical University of Munich, Munich, Germany*
[2]*Faculty of Information Technology and Bionics, Pázmány Péter Catholic University, Budapest, Hungary*
[3]*Chair of Nanoelectronics, Technical University of Munich, Munich, Germany*

(Presented 10 November 2017; received 2 October 2017; accepted 6 October 2017; published online 1 December 2017)

Spin wave (SW) devices are receiving growing attention in research as a strong candidate for low power applications in the beyond-CMOS era. All SW applications would require an efficient, low power, on-chip read-out circuitry. Thus, we provide a concept for an on-chip oscilloscope (OCO) allowing parallel detection of the SWs at different frequencies. The readout system is designed in 40-nm CMOS technology and is capable of SW device characterization. First, the SWs are picked up by near field loop antennas, placed below yttrium iron garnet (YIG) film, and amplified by a low noise amplifier (LNA). Second, a mixer down-converts the radio frequency (RF) signal of 5 − 50 GHz to lower intermediate frequencies (IF) around 10 − 50 MHz. Finally, the IF signal can be digitized and analyzed regarding the frequency, amplitude and phase variation of the SWs. The power consumption and chip area of the whole OCO are estimated to 166.4 mW and 1.31 mm^2, respectively.
https://doi.org/10.1063/1.5007435

I. INTRODUCTION

CMOS has been dominating over decades as a technology for low power, low cost and high-volume applications. In the meantime, more and more emerging devices are getting attention in the research as candidates for beyond-CMOS era.[1] SW based or magnonic devices are considered as a low power alternative to CMOS computing. It can perform both Boolean and non-Boolean operations. A current example of a majority gate, performing logic operations, is demonstrated by Klinger et al.[2] Similar to optical computing,[3] SWs can also perform additional operations using wave phenomena in a more direct way than it is done with Boolean logic.[4] As shown by Csaba[5] and Papp,[6] a non-Boolean computing concept for a Fourier transform calculation can be realized using phase shifting plates.

SW devices operate in a wide GHz frequency range,[4] that makes detection and signal analysis challenging. There are several ways to detect and analyze SW signals, e.g. detection via spin-pumping effect or Brillouin light scattering spectroscopy.[4] But a low power and low cost SW characterization equipment, covering a reasonable frequency range of several GHz, is still missing. Hence, we consider a concept for SW on-chip characterization with respect to their frequency, amplitude and phase variations as published previously in Refs. 7 and 8. In this paper we present a modified SW characterization concept, compared to Ref. 7, with simulation results achieved with a state of the art low power radio frequency (LP-RF) 40-nm CMOS technology. In order to detect smaller SW signal power we split 5 − 50 GHz range in 9 frequency bands. Simulation results for frequency detection as well as for amplitude and phase transfer characteristics are discussed in Sec. III.

[a]Electronic mail: eugen.egel@tum.de

II. CONCEPT FOR ON-CHIP SPIN WAVE DETECTION

In order to convert SWs into electron current, we assume a 50 Ω near field loop antenna placed below the dielectric material yttrium iron garnet (YIG) with low SW propagation damping[4] (see Fig. 1). Based on micro magnetic simulations, an electrical signal power of − 80 to − 90 dBm is expected in the loop antenna, as previously published in Ref. 8. Due to a limited bandwidth of a single on-chip antenna, an array of loop antennas can be used for covering the targeted 5 − 50 GHz frequency range of the SWs, i.e. different frequencies can be picked up by different antennas.[9] Besides, smaller bandwidth of the circuit components provide better noise filtering. Therefore, we assume a slightly reduced signal amplitude of 5 μV in the antenna instead of 15 μV, as previously published in Ref. 7. As known, there is a trade-off between noise figure (NF), chip area and power consumption, which are balanced in the presented design.

The modified OCO is divided in 9 frequency bands, listed in Tab. I. While the mixer is covering the whole frequency range 5 − 50 GHz with the single design, the LNAs and the VCOs are optimized for smaller frequency ranges in order to achieve better performance against noise. For the sake of simplicity, we are currently using near field antennas, but the OCO design works with other SW sensing elements that generate an RF voltage.

Conversion of SWs into electrical signal is perhaps the most challenging aspect of SW devices. One needs a compact, integrable way of measuring SW amplitudes/phases/frequencies and do it without an extensive circuitry that would diminish the advantages of SW devices. The challenges associated with magneto-electric interfaces to SWs are described in Refs. 9 and 10.

As shown in Fig. 1, a periodic radio frequency (RF) signal, picked up by the antenna, is amplified by a differential low noise amplifier (LNA). The ultra-wideband mixer down-converts the signal to lower IF of 10 − 50 MHz. For that purpose, a local oscillator (LO) signal, generated in a voltage controlled oscillator (VCO), is required. Subsequently, an operational amplifier (OpAmp) amplifies the periodic IF signal to higher voltage values. Finally, the amplified signal can be digitized in an analog to digital converter (ADC) that gives information about the SWs frequency, amplitude change and phase variation.

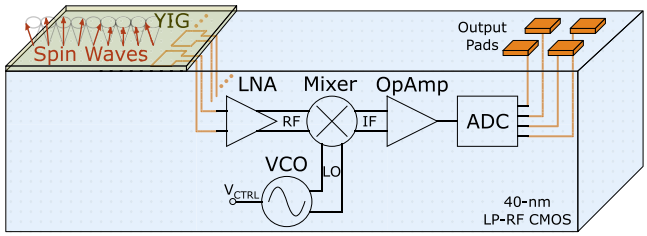

FIG. 1. Block diagram of the on-chip readout circuitry for SW characterization covering 5 − 50 GHz. SWs picked up by inductive loop antennas, placed below the SW low damping medium, e.g. YIG, are amplified and mixed to lower frequencies by 40-nm CMOS circuitry for analyzing the SW frequency, amplitude and phase difference at the output pads.

TABLE I. Frequency bands of the OCO. The check mark symbolizes a single design of the LNA, mixer and VCO covering the corresponding frequency range.

Bands	Freq. Range [GHz]	LNA	Mixer	VCO
1	5 – 9	✓		
2	9 – 13	✓		✓
3	13 – 19	✓		✓
4	19 – 25.5	✓		✓
5	25.5 – 33	✓	✓	✓
6	33 – 39	✓		✓
7	39 – 44			✓
8	44 – 48	✓		✓
9	48 – 50			✓

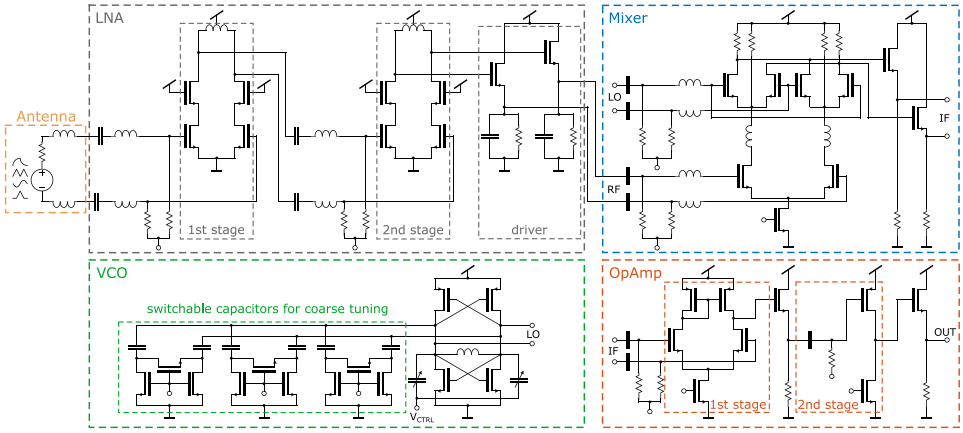

FIG. 2. Equivalent circuit model of the near field loop antenna with the OCO containing differential LNA, mixer, VCO and OpAmp. The LNA has two amplifying stages with an output driver. The LO frequency of the VCO is adjustable with the voltage V_{CTRL} for a fine tuning and with the switchable capacitors for a coarse tuning. The mixer down-converts the signal to lower IFs. Finally, the signal is additionally amplified by the OpAmp with 2 stages.

The topology of the OCO components depicted in Fig. 2 show the design for the frequency band 6 (33 – 39 GHz). The OCO designs of the other bands are very similar to the presented one and skipped for simplicity. In order to amplify – 90 dBm signal of the loop antenna, we use a fully differential LNA with 2 stages. The output driver provides additional isolation between LNA input and output. Besides, the driver is crucial for impedance matching between the LNA output and the mixer input. Starting with the mixer design in Ref. 11, we extended the circuitry with inductors to achieve better NF and higher conversion gain over the whole frequency range of 5 – 50 GHz. To create the IF signal at lower frequencies, the frequency difference of the RF and LO signals should be in the MHz range. Hence, a tunable VCO is necessary for the readout circuitry. Fine tuning of the VCO output frequency is controlled by the voltage V_{CTRL}. For a coarse frequency tuning we use appropriately sized switchable capacitors. The final amplification step is realized with the 2 stage OpAmp bringing IF signal to 100 mV range.

III. SIMULATION RESULTS

The presented results were obtained by simulations using Cadence Virtuoso with device models of the Global Foundries 40-nm LP-RF technology.[12] The simulation results are valid for room temperature of 300 K and already include the noise of each single device. The interconnect parasitics, which will be impacted by the physical layout, have not yet been included in these simulations. The parasitics, extracted from the layout, will of course affect operating frequencies of the OCO. However, this refinement will be tackled in the next project step.

We use transistor models with a low threshold voltage. Implemented resistors operate with silicided or unsilicided p+ poly resistor models, depending on required resistance values. For capacitors we use alternative polarity metal oxide metal capacitors (APMOM Cap) as well as metal isolator metal capacitors (MIM Cap). Symmetric inductor and center tapped inductor models, with nitride as passivation layer, are deployed from optimal inductor finder kit provided by Global Foundries.

The most critical part of the OCO regarding the NF is the first stage of the LNA. Depending on the frequency band, we achieved a NF of the LNAs between 2.4 – 4 dB. For the 50 Ω matching to the antenna, we have a return loss of each LNA better than – 10 dB over the whole frequency range. The achieved gain of the LNAs is around 30 dB (see Fig. 3). We use an active mixer, i.e. the RF signal is additionally amplified during the conversion to lower frequencies. The conversion gain of the mixer is higher than 12 dB as shown in Fig. 3. Finally, the OpAmp amplifies the IF signal with a gain of more than 30 dB in 10 – 50 MHz.

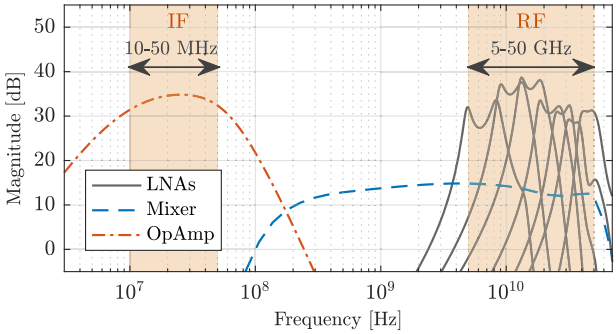

FIG. 3. Simulated gain of the LNAs, mixer and OpAmp. SW signals of 5 – 50 GHz are covered by 7 switchable LNAs with band pass characteristics and amplification of approx. 30 dB. The conversion gain of the mixer is more than 12 dB over the whole frequency range. Down-converted RF signals are amplified by OpAmp with a gain above 30 dB in the IF range from 10 to 50 MHz.

The main task of the OCO is the characterization of the SWs regarding frequency, amplitude and phase variations. The frequency detection is demonstrated in Fig. 4. We assume sinusoidal signals with an amplitude of 10 μV and frequencies at 5, 10, 15, 20, 30, 35, 40, 45, 50 GHz at the input of the OCO in the 9 bands, respectively. Subsequently, the frequency of the LO signal is swept from 5 – 50 GHz. Finally, the simulated signal at the output of the OpAmp is fitted to a sinusoidal curve and divided by the root mean square error (RMSE). As a result, we get peaks at the assumed frequencies (see Fig. 4). Due to a jitter of the LO signal, the resolution of the SW frequency detection is limited. We achieve a precision in frequency of 20 MHz.

The transfer characteristic of the amplitude at the OCO output signal versus input signal is depicted in Fig. 5. Here we use band 6 for demonstration. The RF signal is set to 35 GHz. The LO

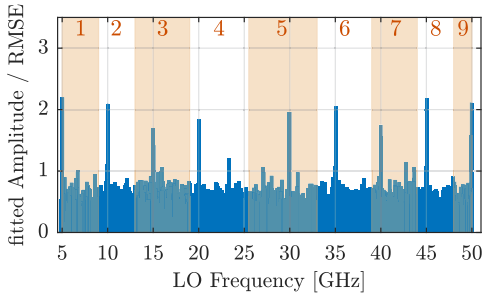

FIG. 4. Frequency detection of the SWs by sweeping the LO frequency in 9 frequency bands, listed in Tab. I. Peaks demonstrate set frequencies at 5, 10, 15, 20, 30, 35, 40, 45, 50 GHz in the loop antennas of 1-9 bands, respectively. The Y-axis represents fitted amplitude of the sinusoidal signal measured at the output of the OpAmp and divided by the RMSE.

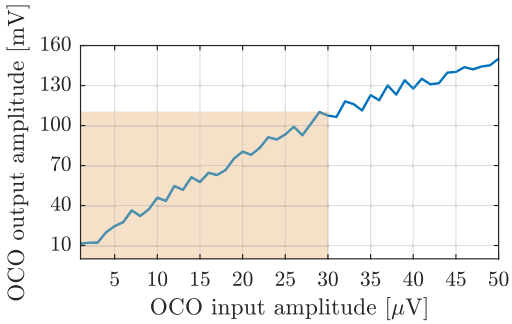

FIG. 5. Amplitude at the OpAmp output by sweeping the amplitude of the voltage in the antenna between 1 – 50 μV with 1 μV steps. Amplitude depedence remain almost linear until 30 μV of the antenna signal.

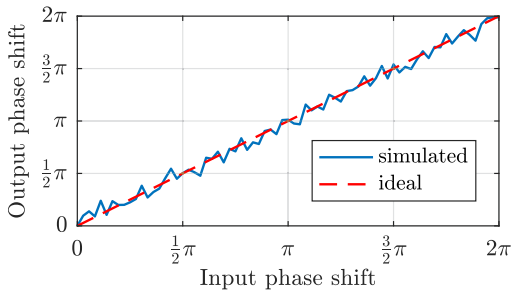

FIG. 6. Phase at the OpAmp output signal dependent on the phase shift of the sinusoidal signal picked up by the antenna. The simulated phase shift curve clearly follows the ideal one.

frequency is set to 35.03 GHz. Due to a limited output voltage swing of the OpAmp, the amplitude curve has a linear characteristic until 30 μV, that corresponds to the assumed maximum signal power of −80 dBm in the loop antenna.[8] The simulation results show that the signal power of less than −96 dBm in the 50 Ω loop antenna is detectable with proposed OCO concept, i.e. a significant improvement of factor 3 compared to our first approach in Ref. 7.

Figure 6 shows the phase transfer characteristic between the input of the OCO and the output of the OpAmp. The phase shift due to run-time of the signal through the circuity is compensated here in order to compare the simulated phase shift with the ideal one. The maximum deviation of the simulated phase shift from ideal one is equal to 23°. The main reason for phase error is the jitter noise of the VCO. An introduction of a phase locked loop (PLL) circuitry in the OCO design could essentially reduce the phase deviation and will be considered in our future work.

IV. CONCLUSION

SW based devices are emerging for high-speed and low power signal processing tasks, but the challenge of an effective SW detection remains. The OCO could be an integrated alternative to current spin wave detecting systems with the near field loop antenna as a sensing element placed below an insulating magnetic medium such as YIG. Besides, the OCO could be adapted for other magneto-resistive or spin hall effect sensing elements.

Simulation results show that the signal power of less than − 96 dBm can be detected with the proposed design. Sensing time for SW amplitude and phase is below 1 μs and for frequency detection less than 40 μs with accuracy of 20 MHz. The OCO shows a further step of a possible realization of the SW on-chip detection with a power consumption of 166.4 mW and chip area of 1.31 mm^2.

ACKNOWLEDGMENTS

Fruitful discussions with S. Kiesel and U. Nurmetov from Technical University of Munich are gratefully acknowledged.

[1] D. E. Nikonov and I. A. Young, "Benchmarking of beyond-CMOS exploratory devices for logic integrated circuits," IEEE Journal on Exploratory Solid-State Computational Devices and Circuits **1**, 3–11 (2015).
[2] S. Klingler, P. Pirro, T. Brächer, B. Leven, B. Hillebrands, and A. V. Chumak, "Design of a spin-wave majority gate employing mode selection," Applied Physics Letters **105**(15), 152410 (2014).
[3] D. C. Feitelson, *Optical Computing: A Survey for Computer Scientists* (MIT Press, 1992).
[4] A. V. Chumak, V. I. Vasyuchka, A. A. Serga, and B. Hillebrands, "Magnon spintronics," Nature Physics **11**(6), 453–461 (2015).
[5] G. Csaba, A. Papp, and W. Porod, "Spin-wave based realization of optical computing primitives," Journal of Applied Physics **115**(17), 17C741 (2014).
[6] A. Papp, W. Porod, E. Song, and G. Csaba, "Wave-based signal processing devices using spin waves," 15th International Workshop on Cellular Nanoscale Networks and their Applications (CNNA), pp. 1–2, 2016.
[7] E. Egel, C. Meier, G. Csaba, and S. Breitkreutz-von Gamm, "Design of a CMOS integrated on-chip oscilloscope for spin wave characterization," AIP Advances **7**(5), 056016 (2017).
[8] S. Breitkreutz-von Gamm, A. Papp, E. Egel, C. Meier, C. Yilmaz, L. Heiß, W. Porod, and G. Csaba, "Design of on-chip readout circuitry for spin-wave devices," IEEE Magnetics Letters **8**, 1–4 (2017).

[9] A. Papp, W. Porod, A. Csurgay, and G. Csaba, "Nanoscale spectrum analyzer based on spin-wave interference," Scientific Reports **7**(9245) (2017).
[10] G. Csaba, A. Papp, and W. Porod, "Perspectives of using spin waves for computing and signal processing," Physics Letters A **381**(17), 1471–1476 (2017).
[11] C.-S. Lin, P.-S. Wu, and H.-Y. Chang, "A 9-50-GHz Gilbert cell down-conversion mixer in 0.13-μm CMOS technology," IEEE Microwave and Wireless Components Letters **16**(5), 293–295 (2006).
[12] Global Foundries, "Product Brief 40nm LP RF Technology," Global Foundries, 2015.